The Chlorinating Behaviour of WCl_6 Towards α-Aminoacids

Marco Bortoluzzi,[a] Fabio Marchetti,[*,b] Maria Grazia Murrali,[b] Guido Pampaloni,[b] and Stefano Zacchini [c]

[a] *University of Venezia Ca' Foscari, Dipartimento di Scienze Molecolari e Nanosistemi, Dorsoduro 2137, I-30123 Venezia.*
[b] *University of Pisa, Dipartimento di Chimica e Chimica Industriale, Via Moruzzi 3, I-56124 Pisa, Italy. Tel: +39 050 2219245. E-mail: fabio.marchetti1974@unipi.it. Webpage: http://www.dcci.unipi.it/fabio-marchetti.html.*
[c] *University of Bologna, Dipartimento di Chimica Industriale "Toso Montanari", Viale Risorgimento 4, I-40136 Bologna, Italy.*

Cl/O interchange took place when WCl_6 was allowed to interact with a series of α-aminoacids. The α-ammonium-acylchloride salts $[\overline{NH_2(CH_2)_3}CHC(O)Cl][WOCl_5]$, **1a**, and $[MeNH_2CH_2C(O)Cl][WOCl_5]$, **1b**, were afforded in *ca.* 55% yields from the reactions of WCl_6 with, respectively, *L*-proline and sarcosine in CH_2Cl_2. By using other reaction media (hexane or $CHCl_3$), the α-amino-acylchloride complexes $WOCl_4[O{=}C(Cl)\overline{CH(CH_2)_3NH_2}]$, **5a**, and $WOCl_4[O{=}C(Cl)CH(R)NHR']$ (R = H, R′ = Me, **5b**; R = R′ = H, **5c**; R = Me, R′ = H, **5d**) were isolated in moderate to good yields from WCl_6 and, respectively, *L*-proline, sarcosine, glycine and *L*-alanine. The formation of **5a,b** is basically the result of HCl release from the parent compounds **1a,b**. **5a** represents a key intermediate in the course of the reaction leading to $(WOCl_4)_2[\mu{:}\kappa^2(O)$-dkp], **2**, dkp = (*S*,*S*)-octahydrodipyrrolo[1,2-*a*:1',2'-*d*]pyrazine-5,10-dione. **2** was optimally prepared from WCl_6/*L*-proline at high temperature conditions. Hydrolytic treatment of **2** afforded the *L*-proline-derived 2,5-diketopiperazine (dkp), finally isolated with an overall yield of 70%. **1a,b** were characterized by X-ray diffractometry, thus providing very rare examples of crystallographically characterized acylchloride derivatives of α-aminoacids. DFT calculations were extensively carried out in order to shed light into structural and mechanistic features.

Introduction

Naturally-occurring α-aminoacids possess attractive properties which have aroused the interest in their employment in synthetic chemistry.[1] Since they are excellent candidates as potential *N,O*-donor ligands, the reactivity of α-aminoacids with transition metal compounds has been largely investigated.[2] α-Aminoacidato derivatives of transition metals have found application in catalytic enantioselective synthesis, both in organic media [3] and in aqueous solution;[1a] moreover they have proved to exhibit interesting behaviour in biological applications [4] and solid state chemistry,[5] and as cytotoxic [6] and sol-gel-derived coating agents.[7] Despite the effort in developing synthetic strategies aimed to incorporate α-aminoacid moieties within metal compounds, very sparse information have appeared in the literature on the interaction of α-aminoacids with high-valent transition metal halides. The formation of coordination adducts was described with reference to the reactions of group 4 tetrachlorides with a restricted series of α-aminoacids, however no unambiguous structural characterization was supplied.[8] The combination of $TiCl_4$ with a variety of α-aminoacids was proposed also as a procedure to obtain crystalline TiO_2.[9] On the other hand, studies on the interaction of α-aminoacids with halides of high-valent elements belonging to groups 5 and 6 are still missing in the literature. This lack of information contrasts with the well-ascertained behaviour of high valent groups 15 and 16 chlorides, *e.g.* PCl_5 [10] and $SOCl_2$,[1,11] generally employed for the functionalization of the carboxylic acid moiety within the α-aminoacid skeleton. In particular, PCl_5 works as a direct Cl-transfer agent toward α-aminoacids, thus allowing the isolation of the relevant α-ammonium-acylchloride salts.[10c] It should be noted that this procedure is generally effective when primary α-aminoacids are involved, conversely it might be problematic with a higher degree of substitution at the nitrogen atom. In the latter case, alternative synthetic pathways usually become operative.[12] Moreover, pyrrolidinium-2-carbonylchloride salts can be easily obtained from PCl_5 and *L*-proline (*i.e.*, a secondary α-aminoacid), but they are unstable at room temperature.

Herein we present a study on the reactivity of WCl_6 with a selection of α-aminoacids (Scheme 1), showing that the former behaves as a direct, effective chlorinating agent toward the carboxylic acid function. The process is effective also with two secondary α-aminoacids, *i.e. L*-proline and sarcosine: the resulting α-(*secondary*)ammonium-acylchloride salts are fairly stable at room temperature and have been crystallographically characterized. Spectroscopic and DFT studies have shed light into structural and mechanistic features, especially regarding the multistep reaction of WCl_6 with *L*-proline, finally yielding the relevant 2,5-diketopyperazine (dkp, see Scheme 1).

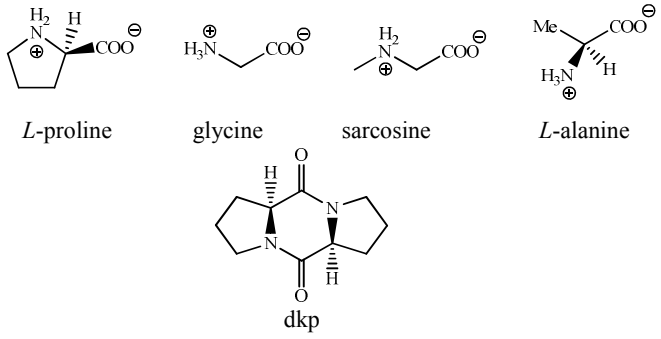

Scheme 1. α-aminoacids discussed in the present work and (*S*,*S*)-octahydrodipyrrolo[1,2-*a*:1',2'-*d*]pyrazine-5,10-dione (dkp).

Results and Discussion

The 1:1 molar reactions of WCl_6, in dichloromethane at room temperature, with *L*-proline and sarcosine afforded the salts $[\overline{NH_2(CH_2)_3}CHC(O)Cl][WOCl_5]$, **1a**, and $[MeNH_2CH_2C(O)Cl][WOCl_5]$, **1b**, as result of Cl/O interchange (Scheme 2).

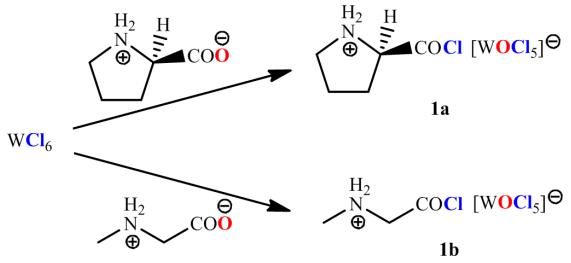

Scheme 2. Synthesis of α-ammonium-acylchloride salts.

Once isolated in the solid state, **1a-b** resulted indefinitely stable at room temperature under inert atmosphere. They were fully characterized by elemental analysis, IR and NMR spectroscopy, moreover crystals suitable for X-ray analysis could be collected from CH_2Cl_2/hexane mixtures stored at −30 °C. The X-ray structures of **1a-b** are shown in Figures 1-2, while relevant bonding parameters are given in Tables 1-2. **1a-b** are ionic compounds containing both the $[WOCl_5]^-$ anion as well as a $[\overline{NH_2(CH_2)_3}CHC(O)Cl]^+$ (**1a**) or $[MeNH_2CH_2C(O)Cl]^+$ (**1b**) cation.

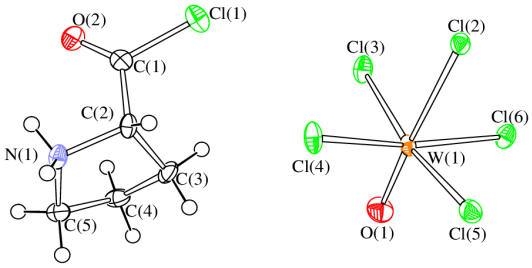

Figure 1. Molecular structure of $[\overline{NH_2(CH_2)_3}CHC(O)Cl][WOCl_5]$, **1a**, with key atoms labeled. Displacement ellipsoids are at the 50% probability level.

Table 1. Selected bond distances (Å) and angles (°) for **1a**.

W(1)–O(1)	1.685(3)	W(1)–Cl(2)	2.5796(11)
W(1)–Cl(3)	2.2931(11)	W(1)–Cl(4)	2.3058(11)
W(1)–Cl(5)	2.3372(11)	W(1)–Cl(6)	2.3347(12)
C(1)–Cl(1)	1.772(5)	C(1)–O(2)	1.177(5)
C(1)–C(2)	1.499(6)	C(2)–C(3)	1.539(6)
C(3)–C(4)	1.515(6)	C(4)–C(5)	1.519(6)
N(1)–C(5)	1.520(6)	N(1)–C(2)	1.525(6)
O(1)–W(1)–Cl(2)	176.77(12)	Cl(4)–W(1)–Cl(6)	169.04(4)
Cl(3)–W(1)–Cl(5)	168.17(4)	Cl(1)–C(1)–O(2)	121.5(4)
Cl(1)–C(1)–C(2)	111.7(4)	C(2)–C(1)–O(2)	126.9(5)
C(1)–C(2)–C(3)	113.4(4)	C(1)–C(2)–N(1)	107.5(4)
C(3)–C(2)–N(1)	103.6(4)	C(2)–C(3)–C(4)	103.8(4)
C(3)–C(4)–C(5)	103.1(4)	C(4)–C(5)–N(1)	103.5(4)
C(5)–N(1)–C(2)	108.5(3)		

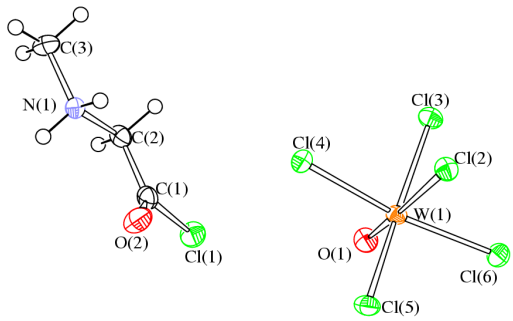

Figure 2. Molecular structure of $[MeNH_2CH_2C(O)Cl][WOCl_5]$, **1b**, with key atoms labeled. Displacement ellipsoids are at the 50% probability level.

Table 2. Selected bond distances (Å) and angles (°) for **1b**.

W(1)–O(1)	1.681(4)	W(1)–Cl(2)	2.6703(14)
W(1)–Cl(3)	2.3206(14)	W(1)–Cl(4)	2.3414(14)
W(1)–Cl(5)	2.2948(13)	W(1)–Cl(6)	2.2920(14)
C(1)–Cl(1)	1.737(6)	C(1)–O(2)	1.188(7)
C(1)–C(2)	1.500(8)	C(2)–N(1)	1.485(7)
C(3)–N(1)	1.490(7)		
O(1)–W(1)–Cl(2)	177.94(14)	Cl(4)–W(1)–Cl(6)	165.73(5)
Cl(3)–W(1)–Cl(5)	166.33(5)	Cl(1)–C(1)–O(2)	122.7(5)
Cl(1)–C(1)–C(2)	112.8(4)	C(2)–C(1)–O(2)	124.5(6)
C(1)–C(2)–N(1)	108.8(4)	C(2)–N(1)–C(3)	114.4(4)

The cations in **1a-b** are rare examples of structurally characterized α-ammonium acylchlorides, and **1b** represents the first case related to sarcosine acylchloride. Bonding distances within the pyrrolidinium ring in **1a** are comparable to those reported for proline hydrochloride [13] and $[\overline{NH_2(CH_2)_3}CHC(O)Cl][MCl_6]$ (M = Nb, Ta).[14] The five-membered cycle possesses an envelope conformation, being N(1), C(2), C(3) and C(5) almost coplanar [mean deviation from the least square plane 0.0358 Å] and C(4) 0.6089 Å away from this plane. The C(1)–O(2) distance [1.177(5) Å] corresponds to an almost pure double bond.[15] The C(2) atom displays an absolute *S* configuration, with absolute structure parameter 0.015(7). An intramolecular hydrogen bond is present involving N(1)–H(11) as a donor and O(2) as an acceptor [N(1)–H(11) 0.891(19) Å; H(11)···O(2) 2.14(4) Å; N(1)···O(2) 2.714(5) Å; N(1)H(11)O(2) angle 121(4)°]. In addition, intermolecular N–H···Cl(W) H-bonds are present [N(1)–H(10) 0.885(19) Å; H(10)···Cl(2)#1 2.300(19) Å; N(1)···Cl(2)#1 3.185(4) Å; N(1)H(10)Cl(2)#1 angle 179(4)°; N(1)–H(11) 0.891(19) Å; H(11)···Cl(2)#2 2.49(4) Å; N(1)···Cl(2)#2 3.190(4) Å; N(1)H(11)Cl(2)#2 angle 136(4)°; symmetry transformations used to generate equivalent atoms: #1 –x+1/2, -y, z-1/2; #2 –x, y+1/2, -z+1/2]. As a result of these intermolecular H-bonds, the cations and the anions are arranged in planes perpendicular to the crystallographic *c* axis (Figure 3), with the anions almost lying on these planes, and the cations just above and below. Only van der Waals contacts are present in between distinct planes.

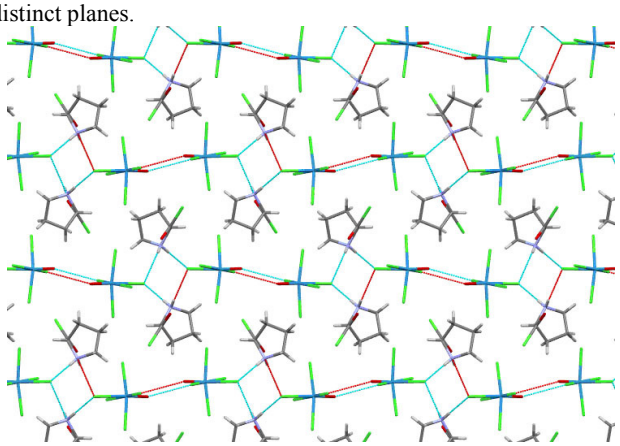

Figure 3. View along the crystallographic *a* axis of the crystal packing of **1a**. The crystallographic *c* axis is vertically oriented. H-bonds are represented as dashed lines.

The $[MeNH_2CH_2C(O)Cl]^+$ cation in **1b** displays bonding parameters very similar to those reported for miscellaneous salts of the $[MeNH_2CH_2C(O)OH]^+$ sarcosinium cation.[16] The C(1)–O(2) interaction [1.188(7) Å] is essentially a double bond, whereas all other contacts are indicative of single bonds.[15]

Intermolecular N–H···Cl(W) H-bonds exist between the cation and the anion of **1b**, resulting in infinite chains [N(1)–H(11) 0.877(19) Å; H(11)···Cl(5)#1 2.34(2) Å; N(1)···Cl(5)#1 3.214(5) Å; N(1)H(11)Cl(5)#1 angle 176(5)°; N(1)–H(12) 0.876(19) Å; H(12)···Cl(5)#2 2.34(2) Å; N(1)···Cl(5)#2 3.202(5) Å; N(1)H(12)Cl(5)#2 angle 168(5)° (Figure 4); symmetry transformations used to generate equivalent atoms: #1 x, y+1, z; #2 –x+1, y+1/2, -z+3/2]. Only van der Waals contacts are present in between distinct planes.

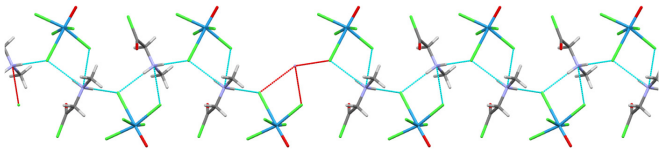

Figure 4. View along the crystallographic *c* axis of the H-bonded infinite chains of cations and anions present in the solid state structure of **1b**. The crystallographic *a* axis is vertically oriented. H-bonds are represented as dashed lines.

The $[WOCl_5]^-$ anion in **1a-b** displays a distorted octahedral geometry. The W(1)–O(1) distances [1.685(3) and 1.681(4) Å for **1a** and **1b**, respectively] are indicative of double bond;[17] as a consequence, the W(1)–Cl(2) interaction [2.5796(11) and 2.6703(14) Å], *trans* to the oxido ligand, is considerably longer respect to the other four W–Cl bonds [ranges 2.2931(11)-2.3347(12) and 2.2920(14)-2.3414(14) Å], suggesting a strong *trans* influence of the oxido ligand. It must be remarked that only four examples of the $[WOCl_5]^-$ anion have been structurally characterized in association with miscellaneous cations,[18] showing similar geometries and bonding parameters. Interestingly, the W–O [1.669-1.823 Å] and *trans* W–Cl [2.474-2.664 Å] distances are spread over a range of values. By comparison of the structures, an inverse correlation between the W–O and the *trans* W–Cl distances can be traced: more precisely, a strengthening of the W–O bond corresponds to a weakening of the *trans* W–Cl interaction. Since the anion is the same in all structures, it is likely that such differences arise from inter-molecular forces and/or packing effects.

The IR spectra of **1a-b** (in the solid state) clearly display the absorptions due to the stretching vibrations of C=O (1771 cm^{-1} in **1a**, 1768 cm^{-1} in **1b**) and W=O (991 cm^{-1} in **1a**, 990 cm^{-1} in **1b**) bonds. The carbonyl absorptions are significantly high-frequency shifted in comparison with the respective situations seen in *L*-proline and sarcosine,[19] as consequence of the conversion of the carboxylic acid function into the acyl-chloride one.

The ^1H and ^{13}C NMR spectra of **1a-b** (in CD_2Cl_2 solutions) exhibit single sets of resonances. Regarding the 2-(methylammonium)acetylchloride cation in **1b**, the *N*-bound protons have been observed as a broad signal at 7.94 ppm, while the ^{13}C carbonyl resonance occurs at 168.5 ppm.

To the best of our knowledge, synthetic procedures to access **1b** have never been reported heretofore.

Although compounds **1a-b** did result stable in the solid state, they could undergo slow transformation in solution. More specifically, we recognized that a CD_2Cl_2 solution of **1a**, contained in a flame-sealed NMR tube, did not change in composition after being stored for 48 h at room temperature. Instead, opening the tube resulted in gas evolution (HCl) and sluggish formation of a green compound. The NMR analyses suggested for the latter the formula $(WOCl_4)_2[\mu{:}\kappa^2(O)\text{-dkp}]$, **2**, comprising a bridging dkp ligand (Schemes 3 and 4). In order to favour the formation of **2**, we tried the 1:1 reaction of WCl_6 with *L*-proline under high temperature conditions: by using toluene as solvent, we recovered **2** in 70% yield after heating at *ca.* 100 °C for 42 h. Compound **2** could be obtained also by two alternative room temperature procedures, *i.e.* from $WOCl_4$/dkp and $WOCl_4$/ $[\overline{NH_2(CH_2)_3CHC(O)Cl}]\,Cl$; the latter reaction was accompanied by HCl release and allowed to isolate **2** with the best yield (82%) (Scheme 3).

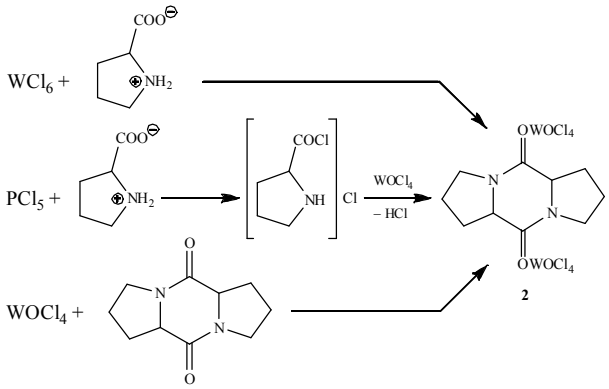

Scheme 3. Reaction pathways to dinuclear complex containing dkp as bridging ligand.

Compound **2** was fully characterized by analytical and spectroscopic techniques. The IR spectrum exhibit a strong absorptions at 1609 cm^{-1}, attributed to the stretching vibration of the carbonyl moieties. The presence of the [W=O] group is manifested by a strong band at 997 cm^{-1}. The NMR spectra (in CD_3CN) show one single set of resonances, in agreement with a symmetrically-coordinated proline-derived frame lacking of *N*-bound hydrogens; the carbonyl groups resonate at 169.6 ppm. The structure of **2** was optimized by DFT calculations and it is shown in Figure 5, while relevant bonding parameters are listed in Table 3.

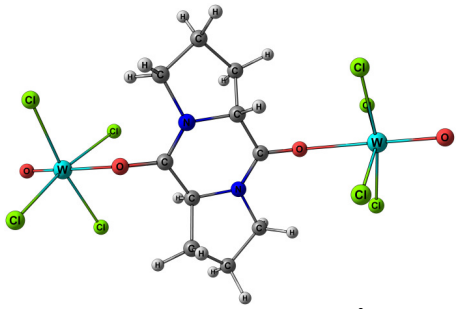

Figure 5. DFT-optimized structure of $(WOCl_4)_2[\mu{:}\kappa^2(O)\text{-dkp}]$, **2**.

Table 3. Selected computed bond distances (Å) and angles (°) for **2**.

	EDF2	M06/C-PCM
W=O	1.683, 1.683	1.660, 1.661
W–Cl	2.336, 2.335	2.347, 2.321
	2.368, 2.370	2.308, 2.342
	2.371, 2.370	2.348, 2.309
	2.311, 2.312	2.341, 2.318
W–OC	2.224, 2.222	2.198, 2.200
C=O	1.254, 1.253	1.257, 1.258
C–N	1.319, 1.319	1.315, 1.316
O=W–OC	177.7, 178.1	177.8, 178.1
O=W–Cl	96.3, 96.4	94.7, 94.8
	94.4, 94.4	95.9, 96.2
	96.9, 97.2	96.4, 96.6
	99.6, 99.4	99.0, 99.2
W–O–C	143.4, 145.2	144.1, 144.7

The treatment of the reaction mixture containing **2** (see Experimental for details) with an aqueous solution of $KHCO_3$ led to the isolation of the *L*-proline-derived cyclic dipeptide (dkp, Scheme 1) with an overall yield of 70% (Scheme 4); dkp was identified by IR [20] and NMR [24b,21] spectroscopy and by GC-MS

analysis. Optical rotation measurement (see Experimental) indicated the retention of configuration respect to the aminoacid precursor. Dkp belongs to the extensive family of 2,5-diketopiperazines, *i.e.* a class of molecules displaying valuable biologic properties [22] and considered as promising scaffolds for drug discovery.[23] Although the 2,5-diketopiperazine skeleton is easily available in nature, being found either alone or embedded in more complex architectures,[23a] there is currently interest in developing new synthetic strategies to obtain it.[23a,24]
The multi-step reaction of WCl_6 with *L*-proline was computationally investigated (Scheme 4).

Insert Scheme 4 about here

Thus we could identify the presumable, elusive species forming at the early stages of the WCl_6/*L*-proline interaction. Monodentate coordination of the carboxylato moiety to the WCl_6 frame appears to be viable, to give the distorted pentagonal bipyramid complex $WCl_6[O{=}C(O)\overline{CH(CH_2)_3NH_2}]$, **3** (Figure 6). The subsequent C–Cl bond formation would take place accompanied by hydrogen migration from N to O, affording the hexacoordinated W-complex $WCl_5[OC(Cl)(OH)\overline{CH(CH_2)_3NH}]$, **4** (Figure 7). The calculated activation free energy for the **3** → **4** conversion resulted low (21.3 kcal mol^{-1}, M06/C-PCM calculations; 15.4 kcal mol^{-1} at EDF2 level). The only imaginary frequency characterizing the transition state geometry (i81 cm^{-1}, M06/CPCM; i80 cm^{-1}, EDF2) accounts at the same time of chloride migration from W to C and of hydrogen transfer from N to O. Salient bonding parameters of the calculated structures of **3**-**4** are provided as Supporting Information (Tables S5-S6).

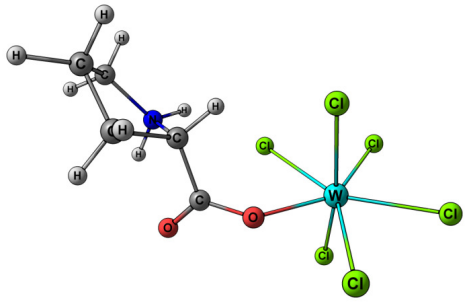

Figure 6. DFT-optimized structure of $WCl_6[O{=}C(O)\overline{CH(CH_2)_3NH_2}]$, **3**.

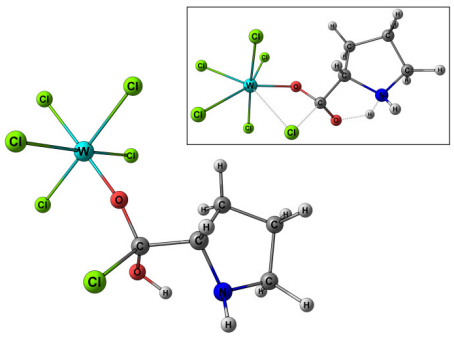

Figure 7. DFT-optimized structure of $WCl_5[OC(Cl)(OH)\overline{CH(CH_2)_3NH}]$, **4**. *Inset*: transition state for the **3**→**4** conversion.

C–O bond breaking in **4** results in the formation of **1a**. Coordinate-driving calculations indicated that this process should have a very low energy barrier. According to the calculations, the conversion of **1a** into **2** is a thermodynamically favoured process by about 24 kcal mol^{-1}; it reasonably takes place with the stepwise elimination of two equivalents of HCl per mole of W. In principle, the first HCl release step might lead to the pyrrolidine-2-carbonylchloride complex $WOCl_4[O{=}C(Cl)\overline{CH(CH_2)_3NH}]$, **5a** (Figure 8, Table S7), *via* the intermediate formation of its hydrochloride salt $\{WOCl_4[O{=}C(Cl)\overline{CH(CH_2)_3NH_2}]\}Cl$, **6** (Figure S11, Table S11 and Scheme 4). The conversion of **1a** into **6** presumably requires the dissociation of one chloride from the $[WOCl_5]^-$ anion; in fact the direct coordination of the organic fragment to $[WOCl_5]^-$ was ruled out, since all the geometry optimizations did not led to stable minima. The ΔG for the reaction $[WOCl_5]^- \rightarrow WOCl_4 + Cl^-$, considering CH_2Cl_2 as implicit solvent, resulted about 16.9 kcal mol^{-1}.

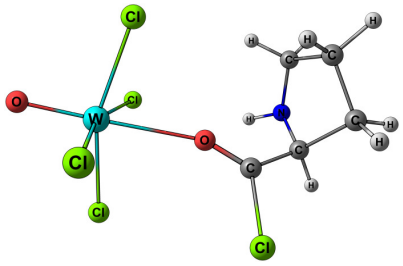

Figure 8. DFT-optimized structure of $WOCl_4[O{=}C(Cl)\overline{CH(CH_2)_3NH}]$, **5a**.

In view of the neutral character of **5a**, we tried to intercept this probable intermediate by using low polar solvents as reaction media. One of these attempts was successful with hexane. The precipitate which formed was characterized by elemental analysis and IR spectroscopy; the outcomes of these characterizations were in agreement with the proposed structure of **5a**. Major feature of the IR spectrum is given by a strong absorption at 1744 cm^{-1}, which is coherent with the presence of a metal-coordinated acylchloride group (the relevant EDF2-calculated IR spectrum displays the carbonyl band at 1733 cm^{-1}). The W=O group has been detected as an intense band at 981 cm^{-1}.
Since the calculated ΔG for the step **1a** → **5a** is high (+8.4 kcal mol^{-1}, Scheme 4), the formation of **5a** appears to be strictly associated with the possibility for the product HCl to escape the reaction site. Coherently with this point, **1a** resulted unchanged in CD_2Cl_2 solution until stored in a close system (see above).
The final conversion of **5a** into **2** is highly favourable from a thermodynamic point of view ($\Delta G_{\mathbf{5a}\rightarrow\mathbf{2}}$ = −32.4 kcal mol^{-1}, Scheme 4). The possibility of isolation of **5a** implies the presence of a quite high activation barrier for the subsequent step. The intermediate compound **7** (Figure S12, Table S12), *i.e.* the species probably forming before the last HCl elimination, has been optimized by means of DFT calculations. The geometry of **7** indicates the presence of a strong intermolecular interaction between [NH] and [C(O)Cl] fragments, possibly driving the formation of **2**.
Compound **1b**, in dichloromethane solution, slowly converted into the α-amino-acylchloride complex $WOCl_4[O{=}C(Cl)CH_2NHMe]$, **5b**, analogous to **5a**. This result was efficiently achieved by 1:1 molar reaction of WCl_6 with sarcosine in $CHCl_3$ (see Experimental). The same procedure allowed to obtain the fairly-stable complexes $WOCl_4[O{=}C(Cl)CH(R)NH_2]$ (R = H, **5c**; R = Me, **5d**) in good yields, respectively from WCl_6/glycine and WCl_6/*L*-alanine (Scheme 4). The reactions were accompanied by HCl formation which was recognized by silver chloride precipitation tests (see Experimental).

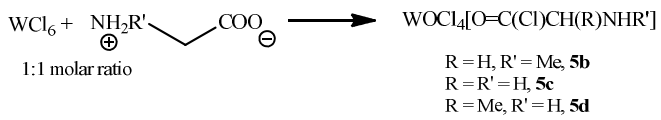

Scheme 4. Synthesis of α-amino-acylchloride complexes.

Compounds **5b-d** were isolated as solid materials which revealed to be almost insoluble in organic solvents. They were characterized in the solid state by elemental analysis and IR spectroscopy. The IR spectra showed the bands due to the [C=O] and [W=O] moieties at typical wavenumber values (*e.g.* at 1730 and 998 cm^{-1}, in the case of **5c**). Our attempts to clearly detect α-ammonium-acylchloride compounds analogous to **1a-b**, in the course of the reactions of WCl_6 with glycine and *L*-alanine, failed. Nevertheless, in principle the formation of α-ammonium-acylchloride salts precedes that of the α-amine-acylchloride complexes **5c-d**. In order to shed light into these aspects, we optimized the DFT structures of **1b** (Figure S2, Table S2), **5b-d** (Figures S8-S10, Tables S8-S10), and the hypothetical compounds $[NH_3CH(R)C(O)Cl][WOCl_5]$ (R = H, **1c**; R = Me, **1d**; Figures S3-S4, Tables S3-S4). The calculated, optimized structures of **5b-d** resemble the one of **5a** in that the organic ligand is located in *trans* position with respect to the oxido moiety; as an example, a view of the DFT structure of **5d** is shown in Figure 9.

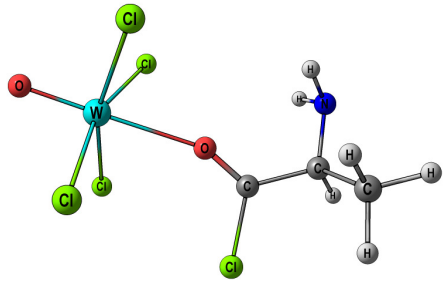

Figure 9. DFT-optimized structure of $WOCl_4[O=C(Cl)CH(CH_3)NH_2]$, **5d**.

According to the calculations, the conversions of **1b-d** into the corresponding **5b-d** are slightly endoergonic reactions which are reasonably driven by HCl elimination.[25]
With the aim of reproducing cyclization reactions analogous to that described for the WCl_6/*L*-proline system, **5b-d** underwent thermal treatment in varying conditions. Notwithstanding all of these attempts afforded mixtures of compounds which could not be identified.

Conclusions

The present paper reports a very rare case of well defined interaction of α-aminoacids with a high valent transition metal halide (WCl_6), the latter working as a selective Cl-transfer agent. The formation of $WOCl_5^-$ α-ammonium acylchloride salts may be considered as the first step of the WCl_6/α-aminoacid interaction, followed by HCl elimination and, in the case of the *L*-proline derived species, clean cyclization reaction. Two secondary α-ammonium acylchloride salts have been isolated as solid materials fairly stable at room temperature.

Experimental

General

1) Materials and methods. *Warning*: all of the metal products reported in this paper are highly moisture-sensitive, thus rigorously anhydrous conditions were required for the reaction and crystallization procedures. The reaction vessels were oven dried at 140°C prior to use, evacuated (10^{-2} mmHg) and then filled with argon. WCl_6 (99.9%, Strem), PCl_5 (98+%, Apollo Sci.) and the α-aminoacids (Apollo Sci.) were commercial products stored under argon atmosphere as received. $WOCl_4$ was prepared according to literature procedure.[26] Once isolated, the metal products were conserved in sealed glass tubes under argon. Solvents (Sigma Aldrich) were distilled from appropriate drying agents under argon atmosphere before use: CH_2Cl_2, CD_2Cl_2 and $CDCl_3$ from P_4O_{10}, toluene from Na, pentane and hexane from $LiAlH_4$. Infrared spectra were recorded at 298 K on a FT IR-Perkin Elmer Spectrometer, equipped with UATR sampling accessory. NMR spectra were recorded on a Bruker Avance DRX400 instrument equipped with BBFO broadband probe at 298 K, unless otherwise stated. The chemical shifts for ^1H and ^{13}C were referenced to the non-deuterated aliquot of the solvent. The chemical shifts for ^{31}P were referenced to external H_3PO_4. The ^1H and ^{13}C NMR spectra were fully assigned *via* ^1H,^{13}C correlation measured through *gs*-HSQC and *gs*-HMBC experiments.[27] GC/MS analysis was performed on a HP6890 instrument, interfaced with MSD-HP5973 detector and equipped with Phenonex Zebron column. Optical rotation measurement was performed with a Perkin–Elmer 141 polarimeter (Na lamp, 589 nm). Carbon, hydrogen and nitrogen analyses were performed on Carlo Erba mod. 1106 instrument. The chloride content was determined by the Mohr method [28] on solutions prepared by dissolution of the solid in aqueous KOH at boiling temperature, followed by cooling down to room temperature and addition of HNO_3 up to neutralization.

2) Synthesis and isolation of $[\overline{NH_2(CH_2)_3CHC(O)Cl}][WOCl_5]$, 1a, and $[MeNH_2CH_2C(O)Cl][WOCl_5]$, 1b. *L*-proline (0.128 g, 1.11 mmol) was added to WCl_6 (0.430 g, 1.08 mmol) in CH_2Cl_2 (15 mL). The mixture was stirred at room temperature for 18 h. Then the resulting dark-green solution was separated from the dark precipitate by filtration. The solution was layered with hexane and stored at –30 °C; a crop of crystals formed in 7 days. Yield 0.099 g, 18%. Additional amount of **1a** was isolated from the reaction precipitate (filtrate): this was washed with toluene (20 mL) and then with pentane (2 x 10 mL), thus it was dried under vacuo. Yield 0.193 g, 35% (total yield 53%).
1a (green solid). Anal. Calcd. for $C_5H_9Cl_6NO_2W$: C, 11.74; H, 1.77; N, 2.74; Cl, 41.57. Found: C, 11.69; H, 1.88; N, 2.65; Cl, 41.32. IR (solid state): 3145m, 3073m-sh, 2956w, 1771s (C=O), 1557s, 1455m, 1369m, 1337m, 1230m, 1208w, 1153m, 1061w, 991vs (W=O), 975s, 941s, 863vs, 832m, 733m cm^{-1}. ^1H NMR (CD_2Cl_2): δ = 8.63 (br, 1 H, NH), 7.71 (br, 1 H, NH), 5.15 (m, 1 H, CH), 3.80 (m, 2 H, NCH_2), 2.79 (m, 1 H, CH_2), 2.46 (m, 1 H, CH_2), 2.35 (m, 1 H, CH_2), 2.21 ppm (m, 1 H, CH_2). $^{13}C\{^1H\}$ NMR (CD_2Cl_2): δ = 172.5 (C=O), 68.4 (CH), 49.0 (NCH_2), 29.5 (CH_2), 23.9 ppm (CH_2).
Compound **1b** was obtained by a procedure similar to that described for the synthesis of **1a**, from WCl_6 (0.360 g, 0.907 mmol) and sarcosine (0.082 g, 0.920 mmol). Yield 0.229 g, 52%. Crystals suitable for X-ray analysis were collected from a CH_2Cl_2 solution layered with hexane and settled aside at –30 °C for 3 d.
1b (ochre-yellow solid). Anal. Calcd. for $C_3H_7Cl_6NO_2W$: C, 7.42; H, 1.45; N, 2.88; Cl, 43.80. Found: C, 7.27; H, 1.50; N, 2.74; Cl, 43.36. IR (solid state): 3015m-br, 2941w-sh, 2803w, 2695w, 1768s (C=O), 1649w, 1567w, 1501w, 1457m, 1434w-m, 1408m, 1348w-m, 1263w, 1169w, 1039w, 1013s, 990vs (W=O), 931vs, 863s, 863s, 817vs, 774vs, 734m cm^{-1}. ^1H NMR (CD_2Cl_2): δ = 7.94 (br, 2 H, NH_2), 4.62 (s-br, 2 H, CH_2), 3.15 ppm (s, 3 H, CH_3). $^{13}C\{^1H\}$ NMR (CD_2Cl_2): δ = 168.5 (C=O), 58.1 (CH_2), 36.2 ppm (CH_3).

3) Synthesis of $(WOCl_4)_2[\mu:\kappa^2(O)$-dkp], 2.
A) From WCl_6/L-proline. WCl_6 (0.360 g, 0.908 mmol), toluene (15 mL) and *L*-proline (0.103 g, 0.895 mmol) were introduced into a Schlenk tube in the order given. The mixture was stirred at 100 °C for 42 hours. The resulting dark precipitate was separated from the supernatant light-brown solution, washed with toluene (2 x 10 mL) and pentane (25 mL), and then dried in vacuo. Yield 0.275 g, 70%. Anal. Calcd. for $C_{10}H_{14}Cl_8N_2O_4W_2$: C, 13.69; H, 1.61; N, 3.19; Cl, 32.32. Found: C, 13.55; H, 1.54; N, 3.29; Cl, 32.10. IR (solid state): 2996vw, 2960vw, 2884vw, 1609vs (C=O), 1487m, 1449w-m, 1341w, 1288w, 1274w, 1232w, 1141w, 1071vw, 997s (W=O), 972m-s, 922w, 904w, 870m, 811w-m, 761m cm^{-1}. ^1H NMR (CD_3CN): δ = 4.32 (m, 1 H, CH), 3.39 (m, 2 H, NCH_2), 2.43 (m, 1 H, CH_2), 2.15 (m, 1 H, CH_2), 2.01 (m, 1 H, CH_2), 1.91 ppm (m, 1 H, CH_2). $^{13}C\{^1H\}$ NMR (CD_3CN): δ = 169.6 (C=O), 60.9 (CH), 49.0 (NCH_2), 29.2 (CH_2), 24.7 ppm (CH_2).
B) From $WOCl_4$/dkp. A suspension of $WOCl_4$ (0.250 g, 0.732 mmol) in CH_2Cl_2 (15 mL) was treated with dkp (0.070 g, 0.360 mmol), freshly prepared from WCl_6/*L*-proline/H_2O (*vide infra*). Progressive turning of the mixture to green occurred. Then the volatile materials were removed, and the residue was rinsed with chloroform (20 mL). Compound **2** was isolated as a green solid and dried in vacuo. Yield 0.190 g, 60%. Anal. Calcd. for $C_{10}H_{14}Cl_8N_2O_4W_2$: C, 13.69; H, 1.61; N, 3.19; Cl, 32.32. Found: C, 13.60; H, 1.49; N, 3.12; Cl, 32.23. IR (solid state): 1612vs (C=O) cm^{-1}.
C) From $WOCl_4$/PCl_5/L-proline. A CH_2Cl_2 solution (15 mL), freshly prepared from PCl_5 (0.225 g, 1.08 mmol) and *L*-proline (0.123 g, 1.07 mmol), was treated with $WOCl_4$ (0.350 g, 1.02 mmol). Immediate formation of an orange solution was noticed. The solution was stirred at room temperature for one week, during which progressive precipitation of a green solid and gas release occurred. Bubbling the gas (HCl) into an aqueous solution of $AgNO_3$ determined the precipitation of a white solid (AgCl). Finally the green solid was isolated from the yellow solution, washed with toluene (2 x 30 mL) and dried in vacuo. Yield 0.367 g, 82%. Anal. Calcd. for $C_{10}H_{14}Cl_8N_2O_4W_2$: C, 13.69; H, 1.61; N, 3.19; Cl, 32.32. Found: C, 13.61; H, 1.69; N, 3.25; Cl, 32.53. IR: 1609vs (C=O) cm^{-1}.

4) Isolation of (*S*,*S*)-octahydrodipyrrolo[1,2-*a*:1',2'-*d*]pyrazine-5,10-dione (dkp). The toluene mixture obtained from the reaction of WCl_6 (0.410 g, 1.03 mmol) with *L*-proline (0.116 g, 1.01 mmol), see above, was allowed to cool to room temperature and treated with a 0.2 M aqueous solution of $KHCO_3$ (25 mL). The resulting mixture was stirred overnight, then the volatile materials were removed. The residue was extracted with acetone (2 x 30 mL), and the organic phase was filtered through a short alumina pad. Hence the solvent was removed, the residue was dissolved in CH_2Cl_2 and charged on a silica column. The use of a mixture of diethyl ether and acetone (1:1 *v*/*v*) as eluent allowed to isolate a fraction corresponding to dkp. The product was afforded as a light-yellow solid upon removal of the volatile materials *in vacuo*. Yield 0.069 g, 70%. Anal. Calcd. for $C_{10}H_{14}N_2O_2$: C, 61.84; H, 7.27; N, 14.42. Found: C, 61.67; H, 7.25; N, 14.21. IR (solid state): 2973w, 2956w, 2883w, 1654vs (C=O),[20] 1512w, 1428s, 1336m, 1292w-m, 1279m, 1259m, 1235w-m, 1202w, 1160m, 1069w, 1020w, 1001w, 920w-m, 802m, 749s, 664m cm^{-1}. ^1H NMR ($CDCl_3$): δ = 4.18 (m, 1 H, CH), 3.52 (m, 2 H, NCH_2), 2.29 (m, 1 H, CH_2), 2.17 (m, 1 H, CH_2), 2.01 (m, 1 H, CH_2), 1.91 ppm (m, 1 H, CH_2). $^{13}C\{^1H\}$ NMR ($CDCl_3$): δ = 166.4 (C=O), 60.4 (CH), 45.2 (NCH_2), 27.7 (CH_2), 23.3 ppm (CH_2). GC-MS: 195 ($[M+1]^+$). $[\alpha]_D^{25}$ = –67 (*c* 1, CH_3OH).[20]

5) Synthesis and isolation of $WOCl_4[O=C(Cl)\overline{CH(CH_2)_3NH}]$, 5a. A suspension of WCl_6 (0.290 g, 0.731 mmol) in hexane (15 mL) was treated with *L*-proline (0.082 g, 0.712 mmol). The mixture was stirred at room temperature for 48 hours. During this period of time the system was purged with argon in order to remove the released gas (HCl). Bubbling the latter into an aqueous solution of $AgNO_3$ determined the precipitation of a white solid (AgCl). A dark-red solid was obtained, which was separated from the supernatant solution and dried in vacuo. Yield 0.118 g, 35%. Anal. Calcd. for $C_5H_8Cl_5NO_2W$: C, 12.64; H, 1.70; N, 2.95; Cl, 37.30. Found: C, 12.58; H, 1.70; N, 3.05; Cl, 37.15. IR (solid state): 2983m, 2881m, 1744vs (C=O), 1557s, 1450m, 1371vs, 1293m, 1220s, 1170m, 1084w, 1034w, 981vs (W=O), 944m, 862s, 844vs, 809vs, 780vs, 722m cm^{-1}.

6) Synthesis and isolation of $WOCl_4[O=C(Cl)CH(R)NHR']$ (R = H, R′ = Me, 5b; R = R′ = H, 5c; R = Me, R′ = H, 5d). *General procedure:* the appropriate α-aminoacid was added to WCl_6 in $CHCl_3$ (15 mL). The mixture was stirred at room temperature for 7 days. During this period of time, the system was purged with argon in order to remove the released gas (HCl). A dark-red solid was obtained, which was separated from the supernatant solution and dried in vacuo. Thus the volatile materials were removed under reduced pressure; the resulting residue was washed with toluene (20 mL) and pentane (20 mL), and then dried in vacuo. The same reactions were conducted in analogous conditions in sealed glass tube; after 1 week, the tube was cooled to *ca.* –40 °C and opened. The released gas (HCl) was conveyed into an aqueous solution of $AgNO_3$, thus determining the precipitation of a white solid (AgCl).
$WOCl_4[O=C(Cl)CH_2NHMe]$, 5b. Yellow solid, 73% yield from WCl_6 (0.460 g, 1.16 mmol) and sarcosine (0.105 g, 1.18 mmol). Anal. Calcd. for $C_3H_6Cl_5NO_2W$: C, 8.02; H, 1.35; N, 3.12; Cl, 39.46. Found: C, 8.10; H, 1.43; N, 3.04; Cl, 39.35. IR (solid state): 3157m, 3111w, 3006, 1727s (C=O), 1596m, 1557m, 1456m, 1428w-m, 1410s, 1259m, 1209m, 1150w-m, 1055w, 979vs (W=O), 937w-m, 894m, 872m, 793vs, 766vs-sh cm^{-1}.
$WOCl_4[O=C(Cl)CH_2NH_2]$, 5c. Green solid, 77% yield from WCl_6 (0.430 g, 1.08 mmol) and glycine (0.083 g, 1.11 mmol). Anal. Calcd. for $C_2H_4Cl_5NO_2W$: C, 5.52; H, 0.93; N, 3.22; Cl, 40.74. Found: C, 5.56; H, 0.88; N, 3.16; Cl, 40.41. IR (solid state): 3139m, 3043m, 2956w, 1730vs (C=O), 1582w, 1499m, 1416m, 1323w, 1304w, 1196vs, 1103m, 1037w, 998vs (W=O), 907s, 852s, 726m-s cm^{-1}.
$WOCl_4[O=C(Cl)CH(Me)NH_2]$, 5d. Green solid, 72% yield from WCl_6 (0.430 g, 1.08 mmol) and *L*-alanine (0.099 g, 1.11 mmol). Anal. Calcd. for $C_3H_6Cl_5NO_2W$: C, 8.02; H, 1.35; N, 3.12; Cl, 39.46. Found: C, 7.98; H, 1.26; N, 3.14; Cl, 39.28. IR (solid state): 3185m-br, 3122m-br, 1747s (C=O), 1589m, 1565w-sh, 1491m, 1460w, 1391m, 1348w, 1213m, 1186s, 1117m-sh, 1101s, 984vs (C=O), 866m, 802s, 757s cm^{-1}.

7) X-ray crystallographic studies. Crystal data and collection details for **1a** and **1b** are listed in Table 4. The diffraction experiments were carried out on a Bruker APEX II diffractometer equipped with a CCD detector and using Mo-Kα radiation (λ = 0.71073 Å). Data were corrected for Lorentz polarization and absorption effects (empirical absorption correction SADABS).[29] The structures were solved by direct methods and refined by full-matrix least-squares based on all data using F^2.[30] All non-hydrogen atoms were refined with anisotropic displacement parameters. All hydrogen atoms were fixed at calculated positions and refined by a riding model, except N-bonded H-atoms which were located in the Fourier map and refined isotropically using the 1.2 fold U_{iso} value of the parent N-atom. N–H distances have been restrained to 0.89 Å (s.u. 0.02).

Insert Table 4 here

8) Computational studies. The computational geometry

optimization of the complexes was carried out without symmetry constrains, using the hybrid DFT EDF2 functional [31] in combination with the LACVP** basis set. The latter is a combination of the 6-31G(d,p) basis set with the LANL2DZ effective core basis set.[32] Further geometry optimization was performed using the hyper-GGA functional M06 [33] in combination with a polarized basis set composed by the 6-31G(d,p) set on the light atoms [34] and the ECP-based LANL2TZ(f) set on the metal centre.[35] C-PCM implicit solvation model (ε = 9.08) was added.[36] In all of the cases the stationary points were characterized by IR simulations, from which zero-point vibrational energies and thermal corrections were obtained.[37] DFT-simulated IR data, obtained with harmonic approximation, assisted the interpretation of experimental IR spectra. Gaussian 09 [38] and Spartan 08 [39] were used as software.

Supporting Information. Figures S1-S12 show the DFT-calculated structures of **1a-d**, **3**, **4**, **5a-d**, **6**, **7**. Tables S1-S12 contain the relevant bonding parameters. The DFT-optimized structures are also collected in a separated *.xyz* file. CCDC reference numbers 993258 (**1a**) and 1038415 (**1b**) contain the supplementary crystallographic data for the X-ray studies reported in this paper. These data can be obtained free of charge at www.ccdc.cam.ac.uk/conts/retrieving.html [or from the Cambridge Crystallographic Data Centre, 12, Union Road, Cambridge CB2 1EZ, UK; fax: (internat.) +44-1223/336-033; e-mail: deposit@ccdc.cam.ac.uk].

References and Notes

1 (a) J. Paradowska, M. Stodulski, J. Mlynarski, *Angew. Chem. Int. Ed.,* 2009, **48**, 4288-4297; (b) A. B. Hughes Ed., *Amino Acids, Peptides and Proteins in Organic Chemistry*, Vol 3, 2011, Wiley-VCH, Weinheim.

2 *See for instance*: (a) D. Desbouis, I. P. Troitsky, M. J. Belousoff, L. Spiccia and B. Graham, Coord. Chem. Rev., 2012, **256**, 897-937; (b) J. Chin, S.-S. Lee, K.-J. Lee, S. Park and D. H. Kim, *Nature*, 1999, **401**, 254-257. (c) K. Severin, R. Bergs, W. Beck, *Angew. Chem. Int. Edit*., 1998, **37**, 1635-1654. (d) M. Hayatifar, F. Marchetti, G. Pampaloni and S. Zacchini, *Inorg. Chem.,* 2013, **52**, 4017-4025. (e) *Comprehensive Coordination Chemistry II*, J. A. McCleverty, T. J. Meyer, Eds, Elsevier Science, 2003. (f) S. H. Laurie, *Amino Acids, Peptides and Proteins*, in *Comprehensive Coordination Chemistry*, G. Wilkinson, R. D. Gillard, J. A. McCleverty, Eds, Pergamon Press, Oxford, 1987, **2**, 739-776.

3 K. Micskei, T. Patonay, L. Caglioti and G. Palyi, *Chem. Biodiv.* 2010, **7**, 1660-1669.

4 (a) A. Wojciechowska, M. Daszkiewicz, Z. Staszak, A. Trusz-Zdybek, A. Bienko and A. Ozarowsk, *Inorg. Chem.*, 2011, **50**, 11532-11542. (b) Y. Pérez, V. Lòpez, L.-R. Rivera, A. Cardona and E. Meléndez, *J. Biol. Inorg. Chem.*, 2005, **10**, 94–110.

5 S. Ding, Y. Wang, Z. Hong, X. Lü, D. Wan and F. Huang, *Chem. Eur. J.* 2011, **17**, 11535-11541. (b) X. Wang, L. Liu, H. Cheng and A. J. Jacobson, *Chem. Commun*., 1999, 2531-2532.

6 R. Hernández, J. Méndez, J. Lamboy, M. Torres, F. R. Román and E. Meléndez, *Toxicol. Vitro,* 2010, **24**, 178-183. (b) M. M. Harding, M. Prodigalidad and M. J. Lynch, *J. Med. Chem*., 1996, **39**, 5012-5016.

7 R. Urlaub, U. Posset and R. Thull, *J. Non-Cryst. Solids,* 2000, **265**, 276-284.

8 N. S. N. Jalil, L. T. Hameed, *Synthesis and Reactivity in Inorganic and Metal-Organic Chemistry*, 1995, **25,** 1633-51.

9 (a) O. Durupthy, J. Bill and F. Aldinger, *Cryst. Growth Design*, 2007, **7**, 2696-2704. (b) O. Durupthy, L. P. H. Jeurgens and J. Bill, *ACS Appl. Mat. Interfaces*, 2011, **3**, 1624-1632.

10 (a) S. Levine, *J. Am. Chem. Soc*., 1954, **76**, 1382. (b) Á. L. Fuentes de Arriba, L. Simón, C. Raposo, V. Alcázar and J. R. Morán, *Tetrahedron*, 2009, **65**, 4841-4845. (c) M. Bortoluzzi, F. Marchetti, M. G. Murrali and G. Pampaloni, *Inorg. Chim. Acta*, 2015, **427***,* 150-154. (d) A. Ookawa and K. Soai, *J. Chem. Soc., Perkin Trans.* **1**, 1987, 1465-1471.

11 (a) S. M. Jones, J. E. Urch, M. Kaiser, R. Brun, J. L. Harwood, C. Berry and I. H. Gilbert, *J. Med. Chem*., 2005, **48**, 5932-5941. (b) E. Bélanger, M.-F. Pouliot and J.-F. Paquin, *Org. Lett.*, 2009, **11**, 2201-2204. (c) A. Nagai, T. Miyagawa, H. Kudo and T. Endo, *Macromolecules*, 2003, **36**, 9335-9339.

12 V. I. Maksimov, *Tetrahedron,* 1965, **21**, 687-698, and references therein.

13 (a) M. E. Kamwaya, O. Oster and H. B. Bradaczek, *Acta Cryst.*, 1981, **B37**, 1391-1393. (b) Y. Mitsui, M. Tsuboi, Y. Iitaka, *Acta Cryst.*, 1969, **B25**, 2182-2192.

14 F. Marchetti, G. Pampaloni and S. Zacchini, *RSC Adv.*, 2014, **4**, 60878-60882.

15 F. H. Allen, O. Kennard, D. G. Watson, L. Brammer, A. G. Orpen, R. Taylor, *J. Chem. Soc., Perkin Trans. 2,* 1987, S1-S19.

16 (a) M. Fleck, V. V. Ghazaryan and A. M. Petrosyan, *Solid State Sci.*, 2012, **14**, 952. (b) R. V. Krishnakumar, M. Subha Nandhini and S. Natarajan, *Acta Crystallogr. C.*, 2001, **57**, 165. (c) M. T. Averbuch-Pouchot, A. Durif and J. C. Guitel, *Acta Crystallogr. C.*, 1988, **44**, 1968. (d) D. Chwaleba, Z. Ciunik, M. M. Ilczyszyn and M. Ilczyszyn, M. *J. Mol. Struct.*, 2006, **791**, 61. (e) V. V. Ghazaryan, M. Fleck, and A. M. Petrosyan, *J. Mol. Struct.*, 2013, **1032**, 35. (f) E. Biavardi, C. Tidisco, F. Maffei, A. Motta, C. Massera, G. G. Condorelli, and E. Delcanale, *Proc. Nat. Acad. Sci. USA*, 2012, **1109**, 2263. (g) M. M. Ilczyszyn, D. Chwaleba, Z. Ciunik, and M. Ilczyszyn, *Chem. Phys.*, 2008, **352**, 57.

17 S. Dolci, F. Marchetti, G. Pampaloni, and S. Zacchini, *Dalton Trans.*, 2013, **42**, 5635-5648.

18 (a) C. A. Dodds, M. D. Spicer, and T. Tuttle, *Organometallics*, 2011, **30**, 6262-6269. (b) N. A. Ovchinnikova, A. E. Sinyakov, V. S. Sergienko, and G. G. Aleksandrov, *Crystallogr. Rep.*, 2003, **48**, 653-656. (c) Y.-J. Lu, and R. H. Beer, *Polyhedron*, 1996, **15**, 1667-1671. (d) P. C. Junk and J. L. Atwood, *J. Chem. Soc., Dalton Trans.*, 1997, 4393-4399.

19 IR (C=O, solid state): 1613vs, 1553vs cm^{-1} (*L*-proline); 1643vs, 1601vs cm^{-1} (sarcosine). IR spectra recorded on solid samples with FT IR-Perkin Elmer Spectrometer equipped with UATR sampling accessory.

20 X. Hu, Z. Shan, and W. Li, *J. Fluorine Chem.*, 2010, **131**, 505-509.

21 N. A. J. C. Furtado, M. T. Pupo, I. Carvalho, V. L. Campo, M. C. T. Duarte and J. K. Bastos, *J. Braz. Chem. Soc.*, 2005, **16**, 1448-1453.

22 (a) M. P. de Carvalho and W.-R. Abraham, *Curr. Med. Chem.*, 2012, **19**, 3564-3577. (b) C. Cornacchia, I. Cacciatore, L. Baldassarre, A. Mollica, F. Felician, and F. Pinnen, *Mini-Rev. Med. Chem.*, 2012, **12**, 2-12.

23 (a) A. D. Borthwick, *Chem. Rev.*, 2012, **112**, 3641-3716. (b) A. S. M. Ressurreição, R. Delatouche, C. Gennari, and U. Piarulli, *Eur. J. Org. Chem.*, 2011, 217-228.

24 (a) H. Thajudeen, K. Park, S.-S. Moon, and I. S. Hong, *Tetrahedron Lett.*, 2010, *51*, 1303-1305. (b) M. Jainta, M. Nieger and S. Bräse, *Eur. J. Org. Chem.*, 2008, 5418-5424. (c) M. Movassaghi, M. Schmidt, and J. A. Ashenhurst, *Angew. Chem. Int. Ed.*, 2008, **47**, 1485-1487.

25 **1b** → **5b** + HCl, ΔG = 5.3 kcal mol^{-1}; **1c** → **5c** + HCl, ΔG = 4.0 kcal mol^{-1}; **1d** → **5d** + HCl, ΔG = 4.1 kcal mol^{-1}.

26 V. C. Gibson, T. P. Kee, and A. Shaw, A. *Polyhedron*, 1990, **9**, 2293-2298.

27 W. Willker, D. Leibfritz, R. Kerssebaum, and W. Bermel, *Magn. Reson. Chem.* 1993, **31**, 287-292.

28 D. A. Skoog, D. M. West, and F. J. Holler, *Fundamentals of Analytical Chemistry,* 7th Edition, Thomson Learning, Inc, USA, 1996.

29 G. M. Sheldrick, *SADABS*, *Program for empirical absorption correction*, University of Göttingen, Göttingen, Germany, 1996.

30 G. M. Sheldrick, *SHELX97*, *Program for crystal structure determination*, University of Göttingen, Göttingen, Germany, 1997.

31 C. Y. Lin, M. W. George, and P. M. W. Gill, *Aust. J. Chem.*, 2004, **57**, 365-370.

32 (a) W. J. Henre, R. Ditchfield, and J. A. Pople, *J. Chem. Phys.*, 1972, **56**, 2257-2261. (b) P. J. Hay, and W. R. Wadt, *J. Chem. Phys.*, 1985, **82**, 270-283. (c) P. J. Hay, and W. R. Wadt, *J. Chem. Phys.*, 1985, **82**, 299-310. (d) M. Dolg, *Modern Methods and Algorithms of Quantum Chemistry*, J. Grotendorst Ed., John Neumann Institute for Computing, NIC series, Jülich, 2000, **1**, 479.

33 Y. Zhao, and D. G. Truhlar, *Theor. Chem. Acc.*, 2008, **120**, 215–241.

34 M. M. Francl, W. J. Pietro, W. J. Hehre, J. S. Binkley, D. J. DeFrees, J. A. Pople, and M. S. Gordon, *J. Chem. Phys.*, 1982, **77**, 3654-3665.

35 L. E. Roy, P. J. Hay, and R. L. Martin, *J. Chem. Theory Comput.*, 2008, **4**, 1029-1031.
36 (a) V. Barone, and M. Cossi, *J. Phys. Chem. A*, 1998, **102**, 1995-2001. (b) M. Cossi, N. Rega, G. Scalmani, V. Barone, *J. Comput. Chem.*, 2003, **24**, 669-681.
37 C. J. Cramer, *Essentials of Computational Chemistry*, 2nd Ed., Wiley, Chichester, 2004.
38 *Gaussian 09*, Revision C.01, M. J. Frisch, et al., Gaussian, Inc., Wallingford CT, 2010.
39 *Spartan '08*, version 1.1.1, Wavefunction, Inc., Irvine CA, 2009. Except for molecular mechanics and semi-empirical models, the calculation methods used in Spartan have been documented in: Y. Shao, et al., *Phys. Chem. Chem. Phys.*, 2006, **8**, 3172–3191.

Scheme 4. Relative free energies of possible intermediates during the synthesis of **2** (M06/C-PCM calculations). Complex **3** was taken as reference (G = 0 kcal mol^{-1}).

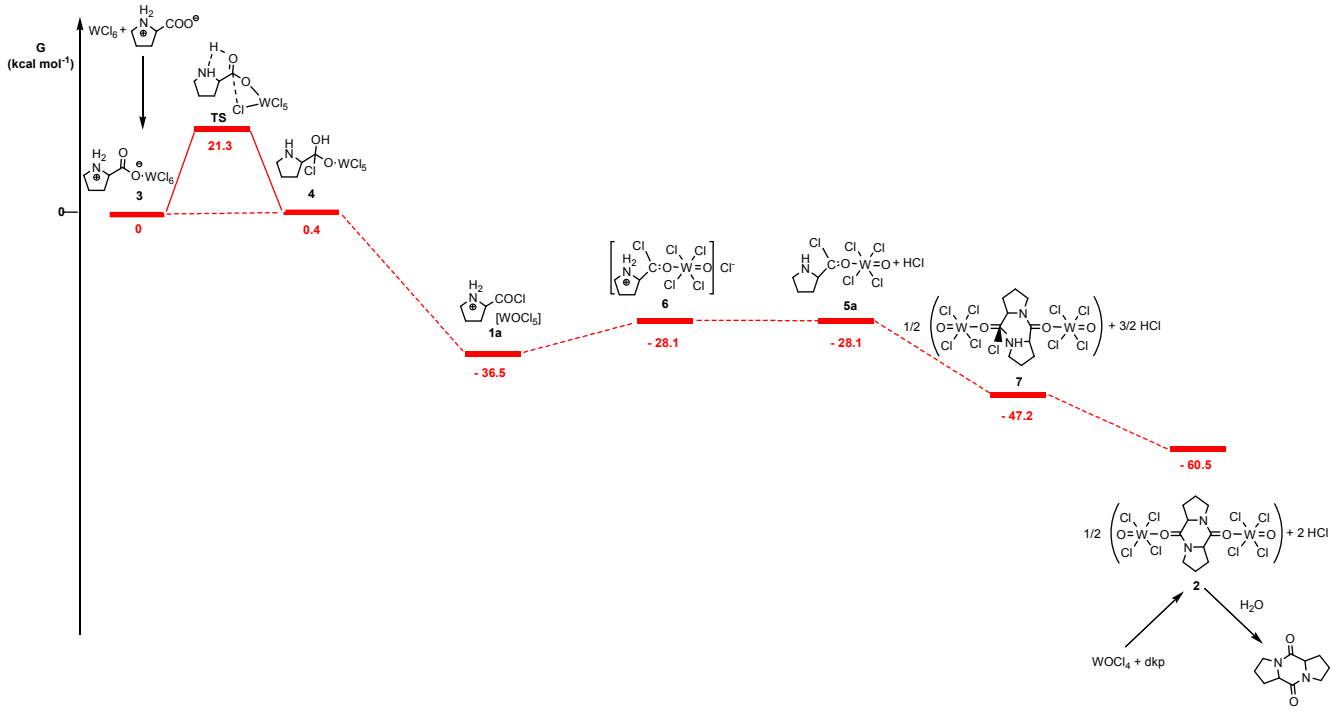

Table 4. Crystal data and experimental details for **1a** and **1b**

	1a	**1b**
Formula	$C_5H_9Cl_6NO_2W$	$C_3H_7Cl_6NO_2W$
Fw	511.68	485.65
T, K	100(2)	100(2)
Crystal system	Orthorhombic	Monoclinic
Space Group	$P2_12_12_1$	$P2_1/c$
a, Å	6.6352(8)	11.0913(14)
b, Å	13.0006(16)	9.9771(13)
c, Å	15.6451(19)	11.5383(15)
β, °	90	105.230(2)
Cell Volume, Å^3	1349.6(3)	1232.0(3)
Z	4	4
D_c, g cm^{-3}	2.518	2.618
μ, mm^{-1}	9.726	10.647
F(000)	952	896
Independent reflections	3260 [R_{int} = 0.0379]	2410 [R_{int} = 0.0417]
Data / restraints / parameters	3260 / 2 / 142	2410 / 2 / 124
Goodness on fit on F^2	1.008	1.003
R_1 ($I > 2\sigma(I)$)	0.0235	0.0276
wR_2 (all data)	0.0463	0.0635
Largest diff. peak and hole, e Å^{-3}	1.185 / –1.596	2.282 / –1.010
Absolute structure parameter	0.015(7)	-